Supporting Information

Experimental and Theoretical Evidences for Low-Lying Excited States in $[Cr_6E_8(PEt_3)_6]$ (E = S, Se, Te) Cluster Molecules

Patrick Bügel,[a] Ivo Krummenacher,[b] Florian Weigend,[c] Andreas Eichhöfer,[d,e*]

[a] P. Bügel, Institut für Nanotechnologie, Karlsruher Institut für Technologie (KIT), Campus Nord, Hermann-von-Helmholtz-Platz 1, 76344 Eggenstein-Leopoldshafen, Germany

[b] Dr. I. Krummenacher, Institut für Anorganische Chemie, Universität Würzburg, 97074 Würzburg, Germany

[c] Prof. Dr. F. Weigend, Fachbereich Chemie, Universität Marburg, 35032 Marburg, Germany

[d] Dr. A. Eichhöfer, Institut für Nanotechnologie, Karlsruher Institut für Technologie (KIT), Campus Nord, Hermann-von-Helmholtz-Platz 1, 76344 Eggenstein-Leopoldshafen, Germany

Tel. 49-(0)721-608-26371

Fax: 49-(0)721-608-26368

e-mail: andreas.eichhoefer@kit.edu

[e] Karlsruhe Nano Micro Facility (KNMF), Hermann-von-Helmholtz-Platz 1, 76344 Eggenstein-Leopoldshafen, Germany

Content

Figure S20 Theoretical electronic spectra of the closed shell and excited state of **2** compared to the experimental ones.

List of compounds

1a $[Cr_6S_8(PEt_3)_6]*1.5\ C_4H_8O$

1b $[Cr_6S_8(PEt_3)_6]$

2a $[Cr_6Se_8(PEt_3)_6]*1.5\ C_4H_8O$

2b $[Cr_6Se_8(PEt_3)_6]$

3 $[Cr_6Te_8(PEt_3)_6]$

Table S1. Crystallographic data for $[Cr_6S_8(PEt_3)_6]$*1.5C_4H_8O (**1a**), $[Cr_6S_8(PEt_3)_6]$ (**1b**), $[Cr_6Se_8(PEt_3)_6]$*1.5C_4H_8O (**2a**) and $[Cr_6Se_8(PEt_3)_6]$ (**2b**) and $[Cr_6Te_8(PEt_3)_6]$ (**3**).

		1a	**1b**	**2a**	**2b**	**3**
sum formula		$C_{36}H_{90}Cr_6P_6S_8$ + (solvent)	$C_{36}H_{90}Cr_6P_6S_8$	$C_{36}H_{90}Cr_6P_6Se_8$ + (solvent)	$C_{36}H_{90}Cr_6P_6Se_8$	$C_{36}H_{90}Cr_6P_6Te_8$
fw [g/mol]		1277.37	1277.37	1652.57	1652.57	2041.69
T [K]		180(2)	180(2)	180(2)	180(2)	150(2)
crystal system		trigonal	triclinic	trigonal	triclinic	monoclinic
space group		*R*–3	*P*–1	*R*–3	*P*–1	*I*2/*a*
Cell	*a* [pm]	1709.70(4)	1178.92(4)	1728.9(2)	1194.06(5)	1342.2(3)
	b	1709.70(4)	1262.30(5)	1728.9(2)	1278.68(5)	1968.0(4)
	c	1943.78(8)	2022.22(7)	1954.4(4)	2021.65(8)	2413.5(5)
	α	90	88.924(3)	90	88.733(3)	90
	β [°]	90	87.547(3)	90	87.029(3)	101.00(3)
	γ	120	72.177(3)	120	71.591(3)	90
V [10^6pm^3]		4920.6(3)	2862.3(2)	5058.9(17)	2924.7(2)	6186(3)
Z		3	2	3	2	4
d_c [g cm^{-3}]		1.293	1.482	1.627	1.877	2.192
$\mu(\lambda)$ [mm^{-1}]		1.382	1.584	5.414	6.243	6.781
F[000]		2004	1336	2436	1624	3824
cryst.size [mm^3]		0.4 × 0.217 × 0.09	0.25 × 0.21 × 0.18	0.18 × 0.13 × 0.12	0.36 × 0.287 × 0.24	0.11 × 0.10 × 0.09
λ [Å]		0.71073	0.71073	0.71073	0.71073	synchrotron (0.80000)
2θ range [°]		3.5–53.5	4.0–70.5	4.7–53.5	3.4–53.5	3.0–65
meas reflns		12770	65054	10660	28738	17437
unique reflns		2321	23669	2377	12347	6965
R_{int}		0.0703	0.0693	0.0628	0.0578	0.0391
reflns with $I > 2\sigma(I)$		1999	17188	2129	9980	6574
restrs / params		0 / 88	0 / 523	0 / 88	0 / 523	0 / 262
$R1(I > 2\sigma(I))$[a]		0.0266	0.0327	0.0236	0.0366	0.0270
*wR*2(all data)[b]		0.0733	0.0744	0.0657	0.0916	0.0718
Solvent mask / e^- per formula unit		109		93.7		
Diff Peak/hole [eÅ^{-3}]		0.41 / –0.63	0.73 / –0.89	0.59 / –0.73	1.01 / –1.69	0.92 / –1.22
CCDC No.						

[a] $R1 = \Sigma||F_o| - |F_c||/\Sigma|F_o|$. [b] $wR2 = \{\Sigma[w(F_o^2 - F_c^2)^2] / \Sigma[w(F_o^2)^2]\}^{1/2}$

Table S2. Crystallographic Data for $[Cr_6E_8(PEt_3)_6]$ (E = S, Se) cluster molecules from literature [a,b]

			$[Cr_6S_8(PEt_3)_6] \cdot 2\ C_6H_6$	$[Cr_6Se_8(PEt_3)_6] \cdot 2\ C_6H_6$	$[Cr_6Se_8(PEt_3)_6]$ [c]	$[Cr_6Se_8(H)(PEt_3)_6] \cdot 2$ thf	$[Cr_6Se_8(PEt_3)_6]$ [c]
ref			[a]	[a]	[a]	[b]	[b]
T [K]			*not given*	*not given*	*not given*	293	226
crystal system			trigonal	trigonal	triclinic	trigonal	triclinic
space group			*R*–3	*R*–3	*P*–1	*R*–3	*P*–1
Cell	*a*	[pm]	1730.1(3)	1751.1(8)	1204.1(2)	1738.4(4)	1206.1
	b				1288.8(2)		1288.7
	c		1974.0(2)	1996.0(7)	2039.8(2)	1976.8(4)	2031.8
	α				88.84(1)		88.58
	β	[°]			87.02(2)		86.76
	γ				71.43(1)		71.75
V [10^6pm^3]			5116.7(13)	5301(4)	2996.6(13)	5173(2)	2994.3

[a] K. Tsuge, H. Imoto, T. Saito, *Bull. Chem. Soc. Jpn.* **1996**, *69*, 627.

[b] S. Kamiguchi, H. Imoto, T. Saito, *Inorg. Chem.* **1998,** *37*, 6852-6857.

[c] data from literature were transformed for comparative reason from the non-conventional setting to a conventional setting

Table S3. Mean atomic distances and standard deviations [pm] in a) **1b** and b) **2b** measured at 120, 200 and 280 K [a]

		exp			
		120 K	200 K	280 K	Δ
1b	d Cr–P	241.26±0.43	241.52±0.41	241.75±0.40	0.49
	d Cr–S	233.50±0.54	233.65±0.45	233.81±0.41	0.31
	d Cr···Cr	256.74±0.73	258.66±0.86	261.20±0.79	4.46
	d S···S	329.34±0.95	329.42±0.86	329.47±0.76	0.13
2b	d Cr–P	241.89±0,38	242.16±0.43	242.57±0.24	0.68
	d Cr–Se	244.56±0,54	244.85±0.48	245.19±0.39	0.63
	d Cr···Cr	263.55±0,68	265.45±0.73	268.14±0.67	4.59
	d Se···Se	345.24±0,73	345.53±0.71	345.91±0.72	0.67

[a] calculated as the sum over all distances divided by the number of distances

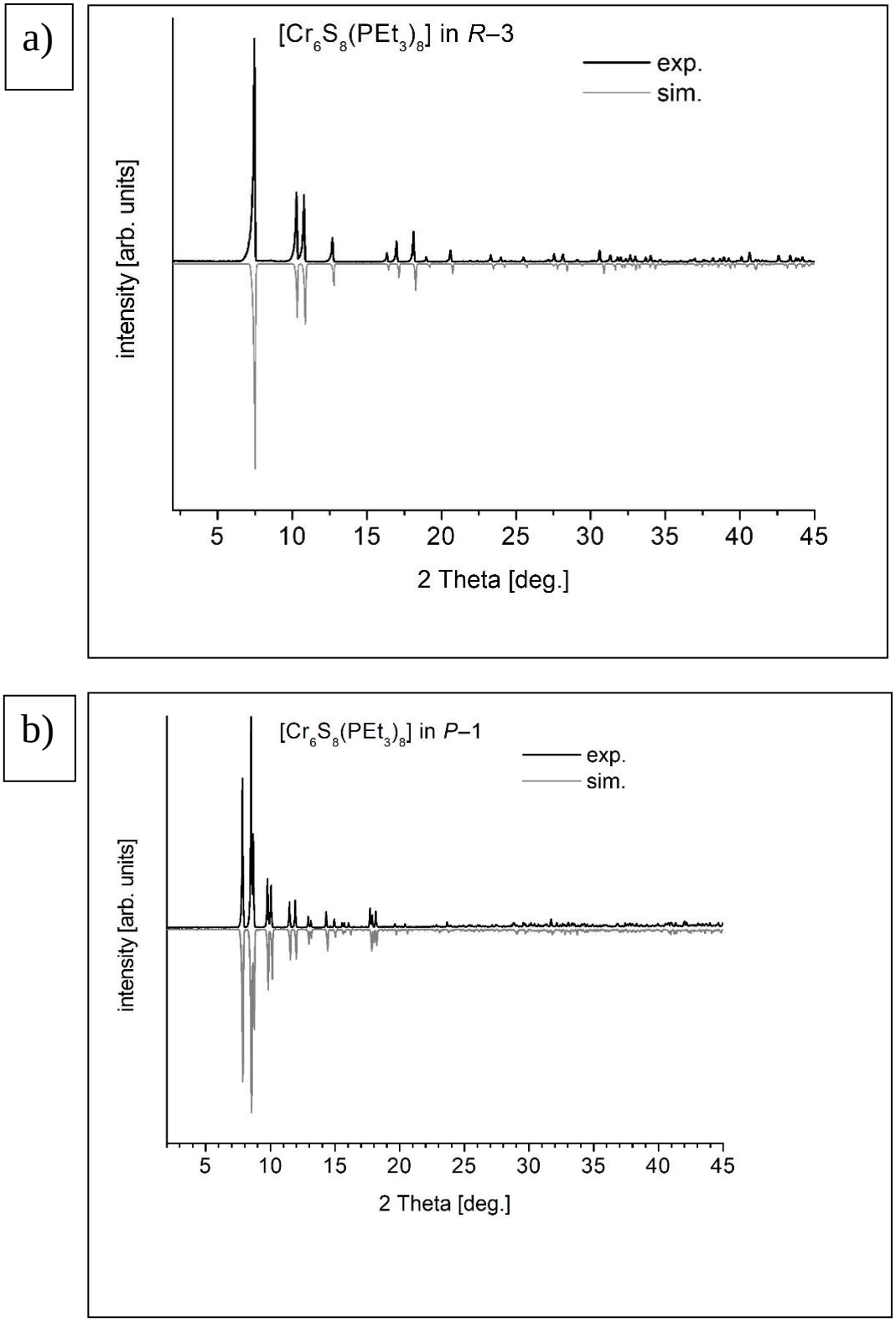

Figure S1. Measured (black) and simulated (grey) X–ray powder patterns ($CuK_{\alpha 1}$) for a) **1a** and b) **1b** (measured as a dried crystalline powder).

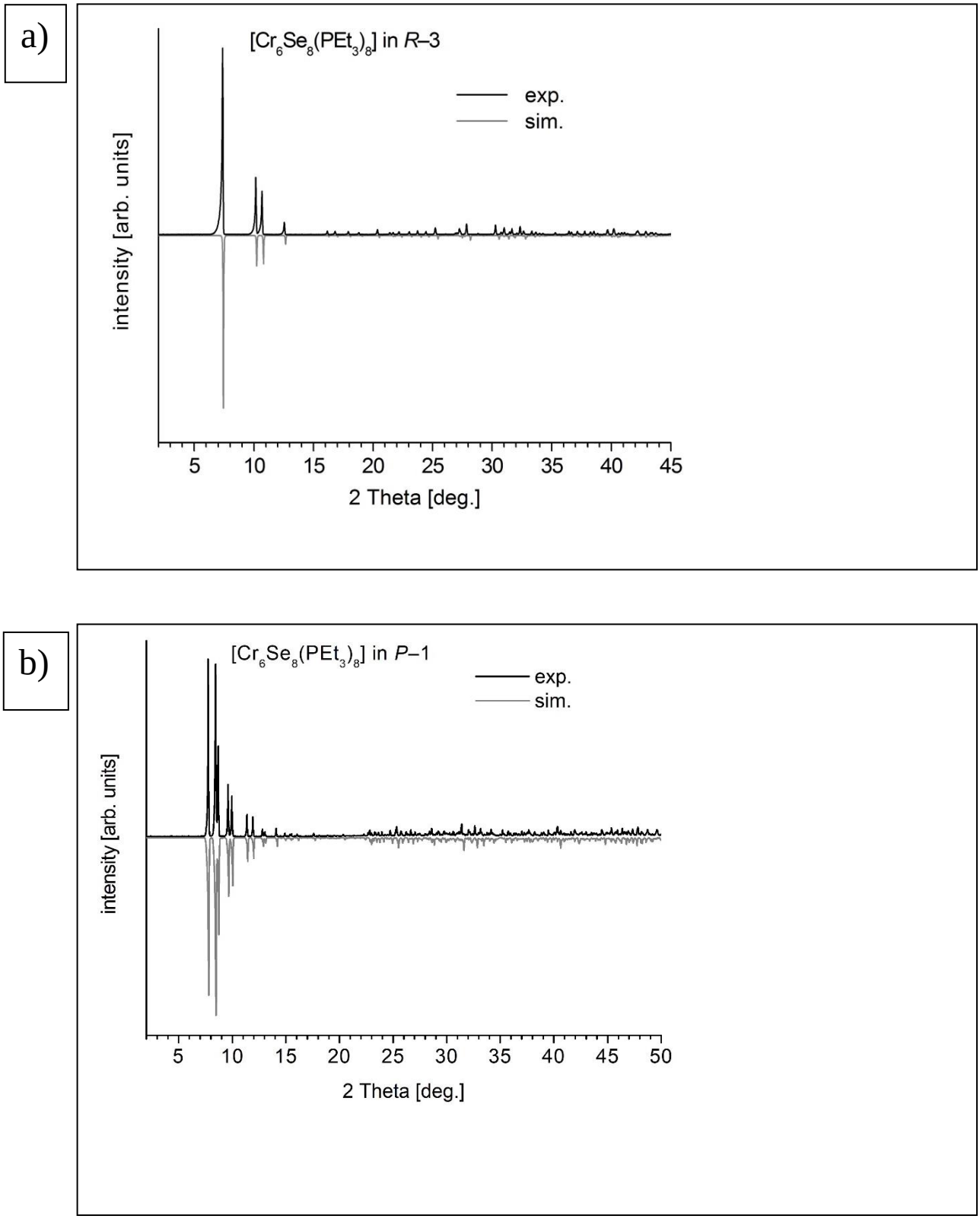

Figure S2. Measured (black) and simulated (grey) X–ray powder patterns ($CuK_{\alpha 1}$) for a) **2a** and b) **2b** (measured as a dried crystalline powder).

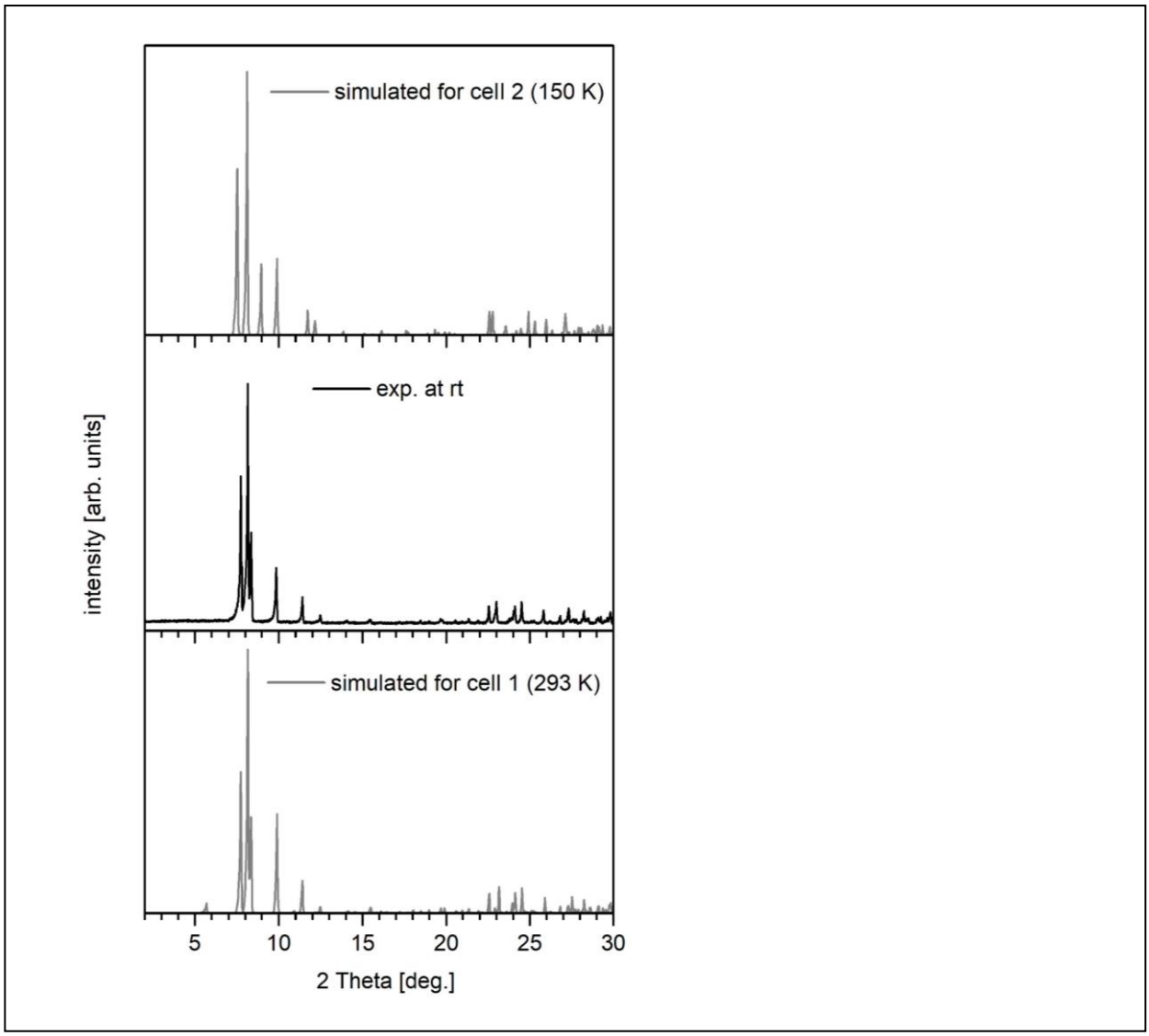

Figure S3. Measured (black) and simulated (grey) X–ray powder patterns ($CuK_{\alpha 1}$) for **3** (measured as a dried crystalline powder). Simulations are performed for cell 1 obtained from single crystal XRD at 293 K (B. Hessen, T. Siegrist, T. Palstra, S. M. Tanzler, M. L. Steigerwald, *Inorg. Chem.*, **1993**, *32*, 5165-5169) and cell 2 obtained from single crystal XRD at 150 K in this work.

.

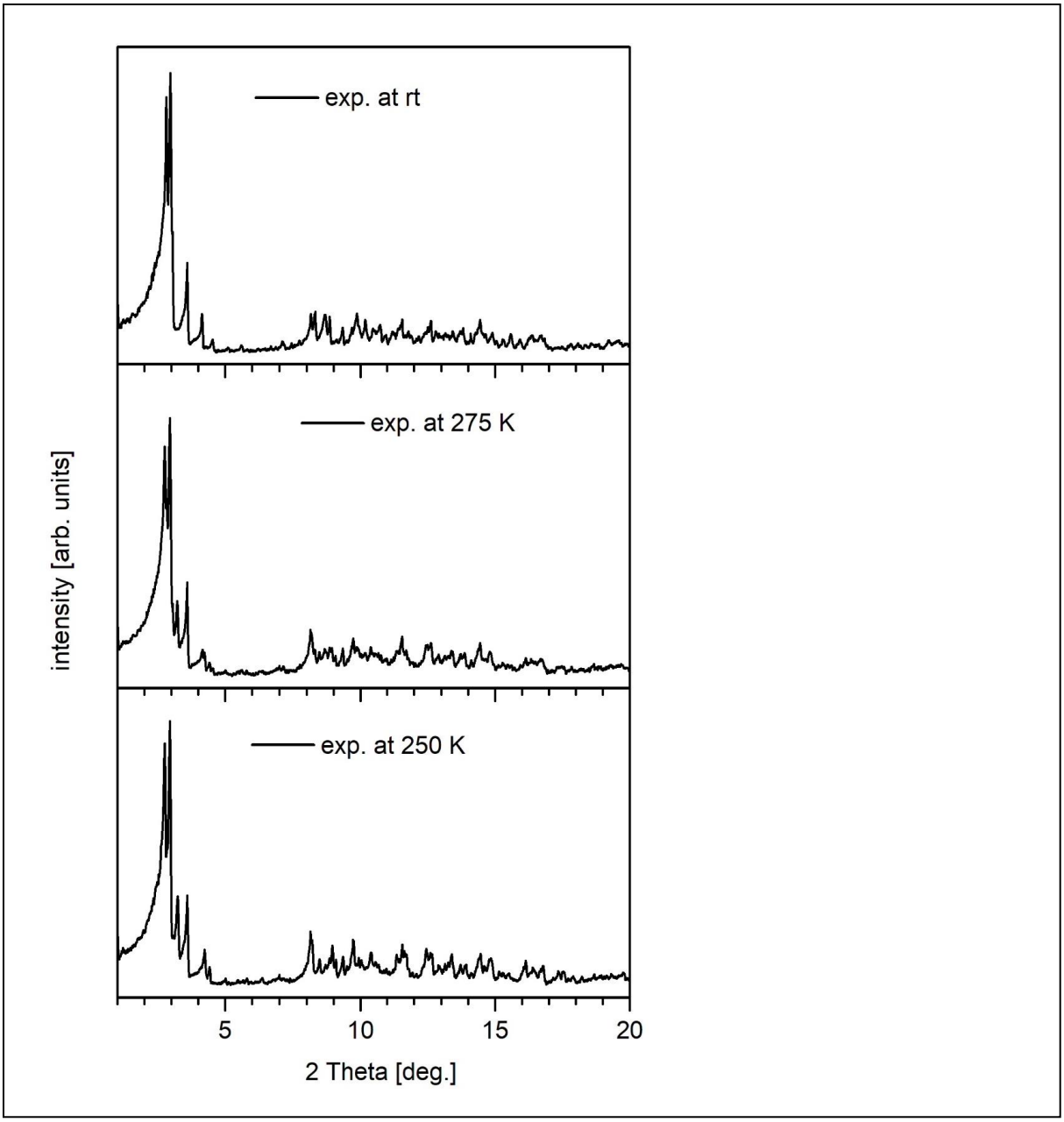

Figure S4. Temperature-dependent X–ray powder patterns ($AgK_{\alpha 1}$) for **3** (measured as a dried crystalline powder).

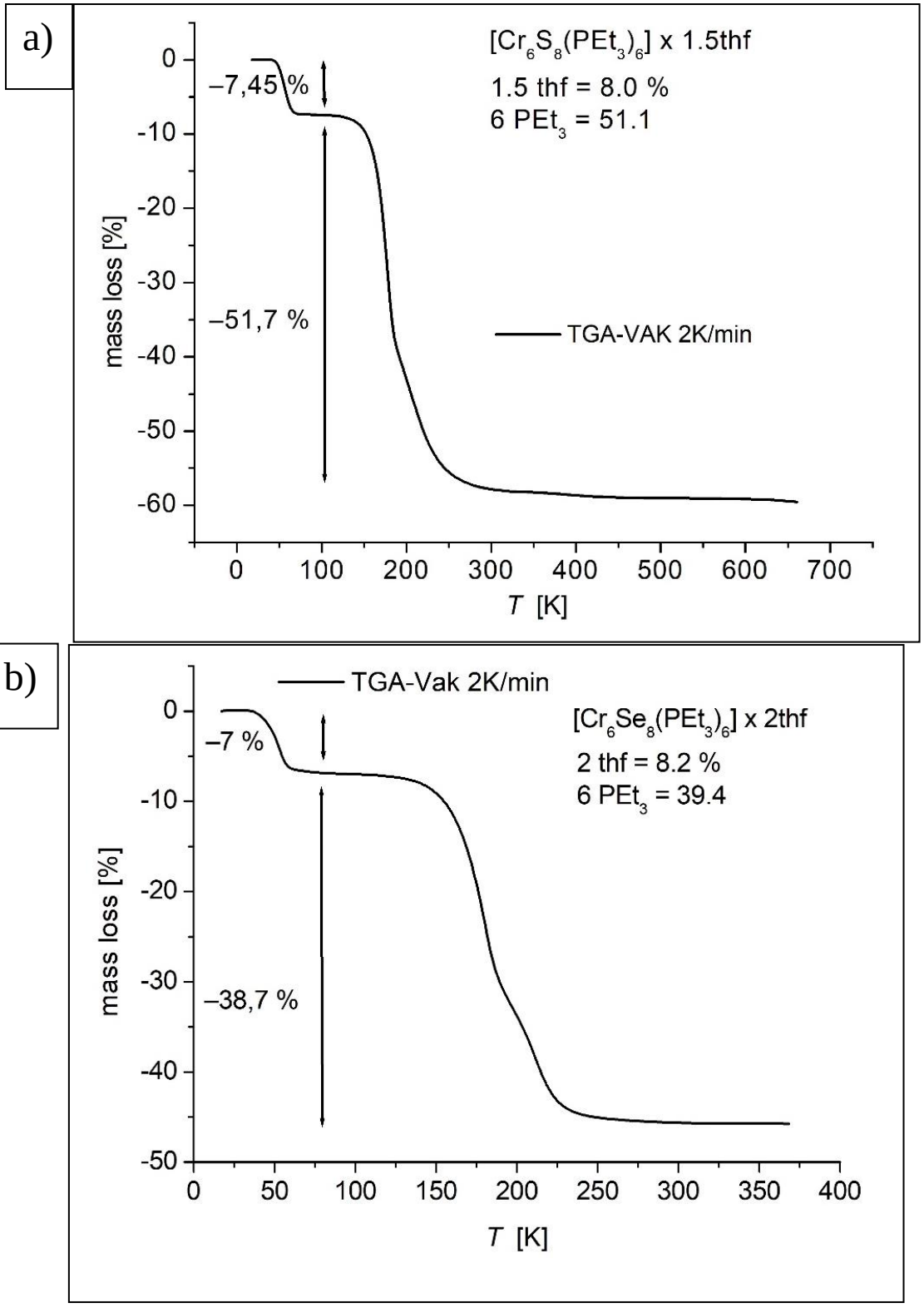

Figure S5 Thermogravimetric analysis of a) **1a** and b) **2a** under vacuum (10^{-3} mbar).

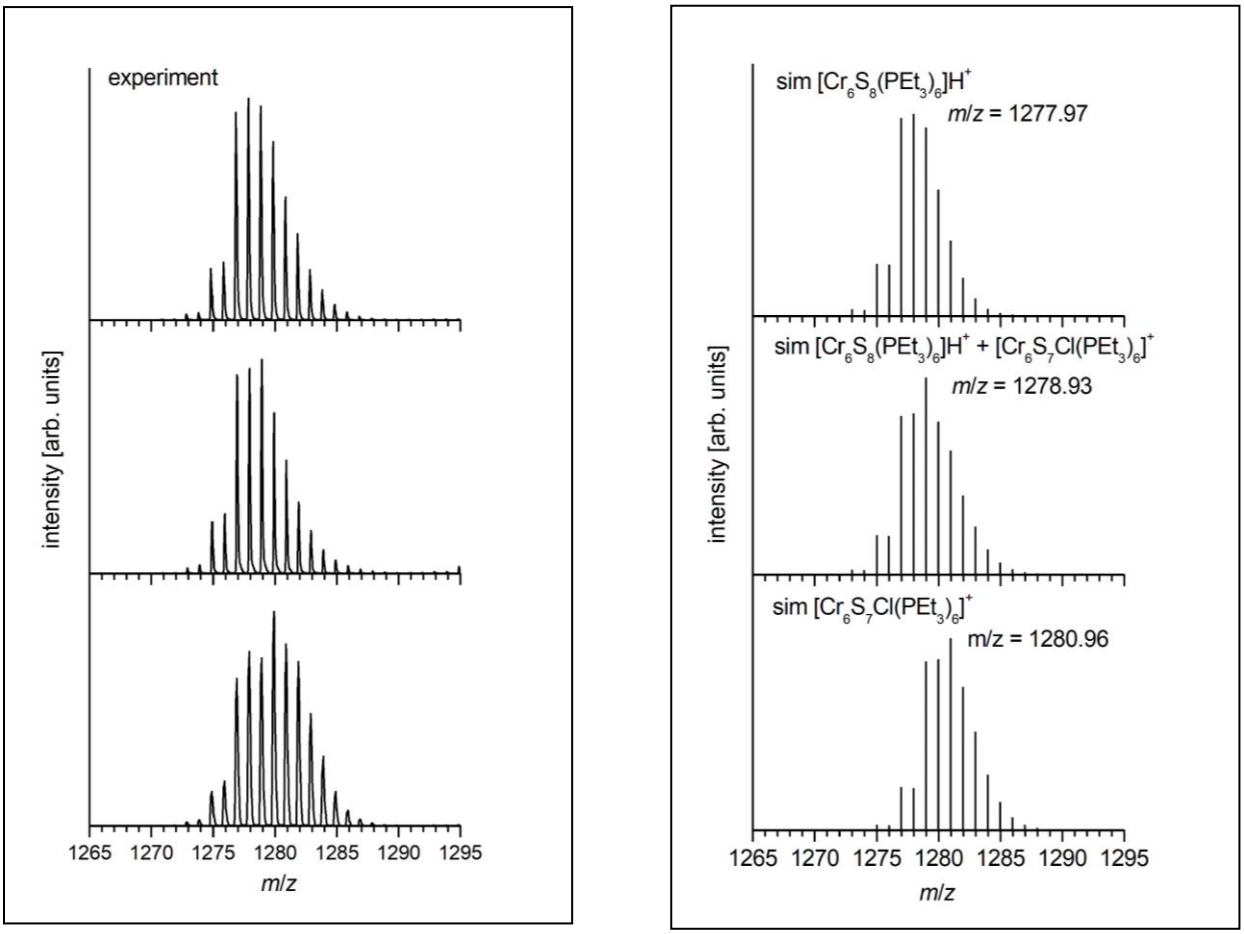

Figure S6. a) Variation of the molecular ion peak of the ESI-ToF mass spectra of **1a** dissolved in toluene upon change of time, b) simulation of the respective molecular ion peaks for different cluster fragments of **1a**.

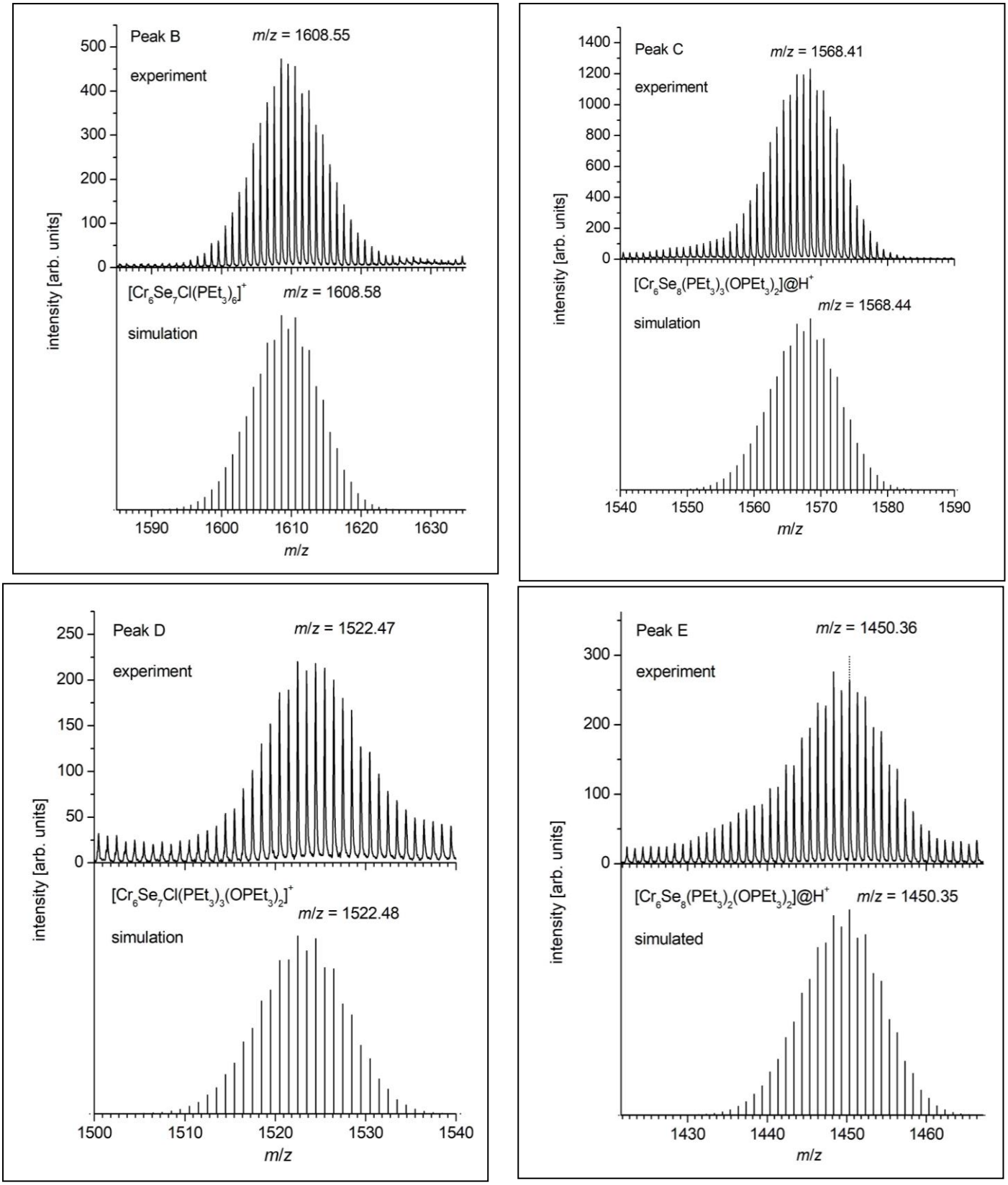

Figure S7. Experimental and simulated molecular fragment ion peaks B – E of the ESI-ToF mass spectra of **2a** dissolved in toluene.

a)

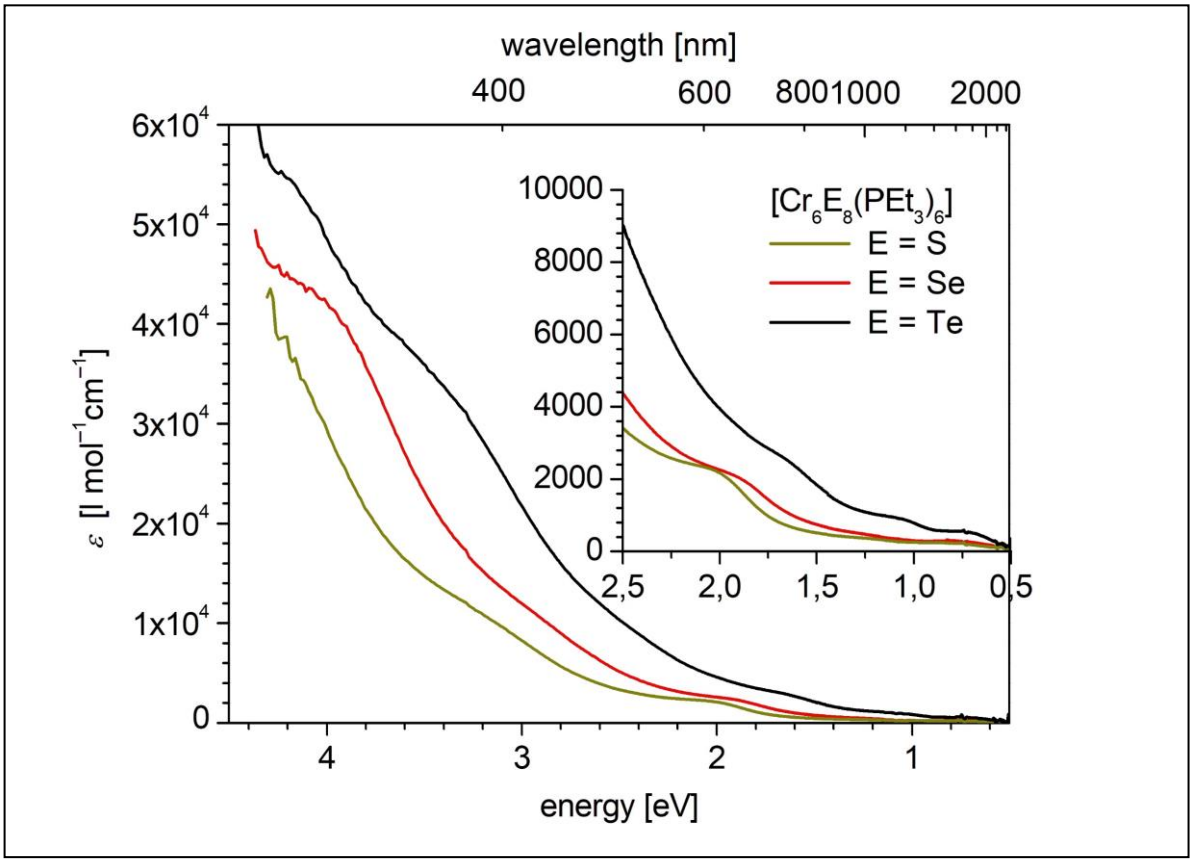

b)

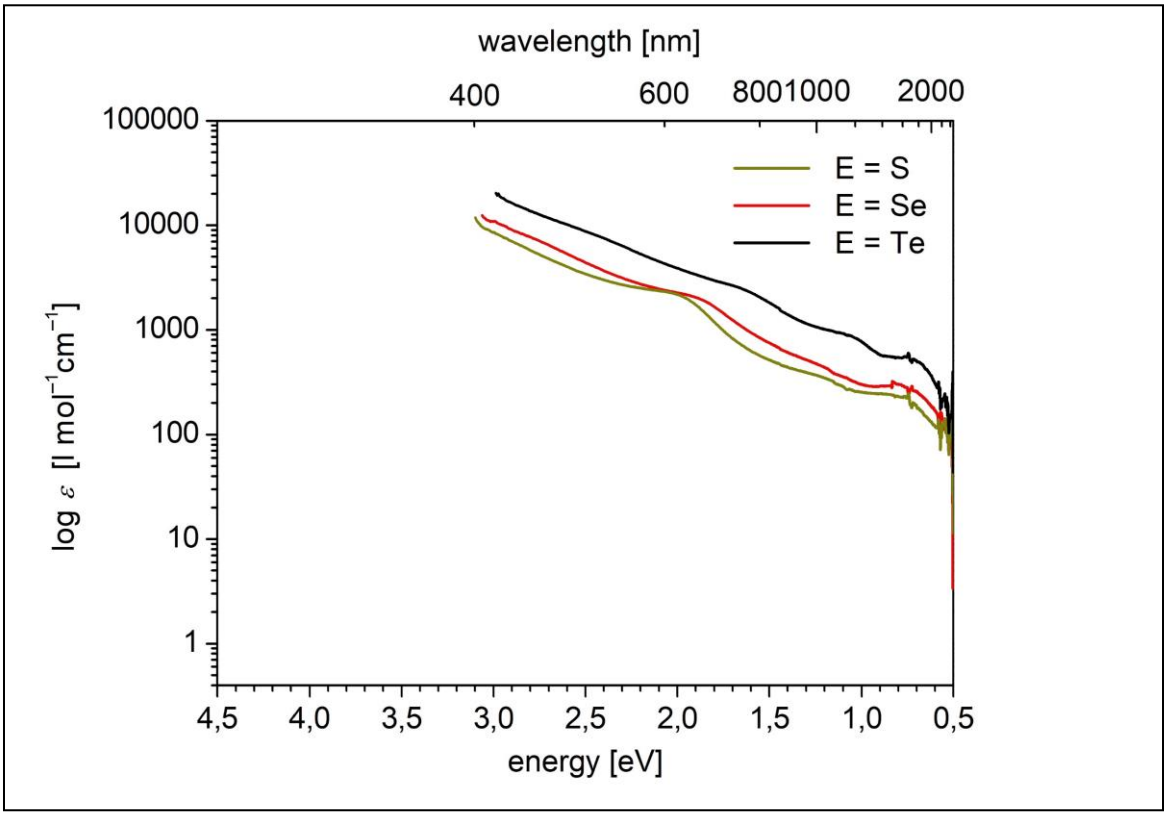

Figure S8. UV-Vis NIR spectra of **1a**, **2a** and **3** in toluene a) for dilute and concentrated (incept) solutions on a linear scale and b) for concentrated solutions plotted on a log scale.

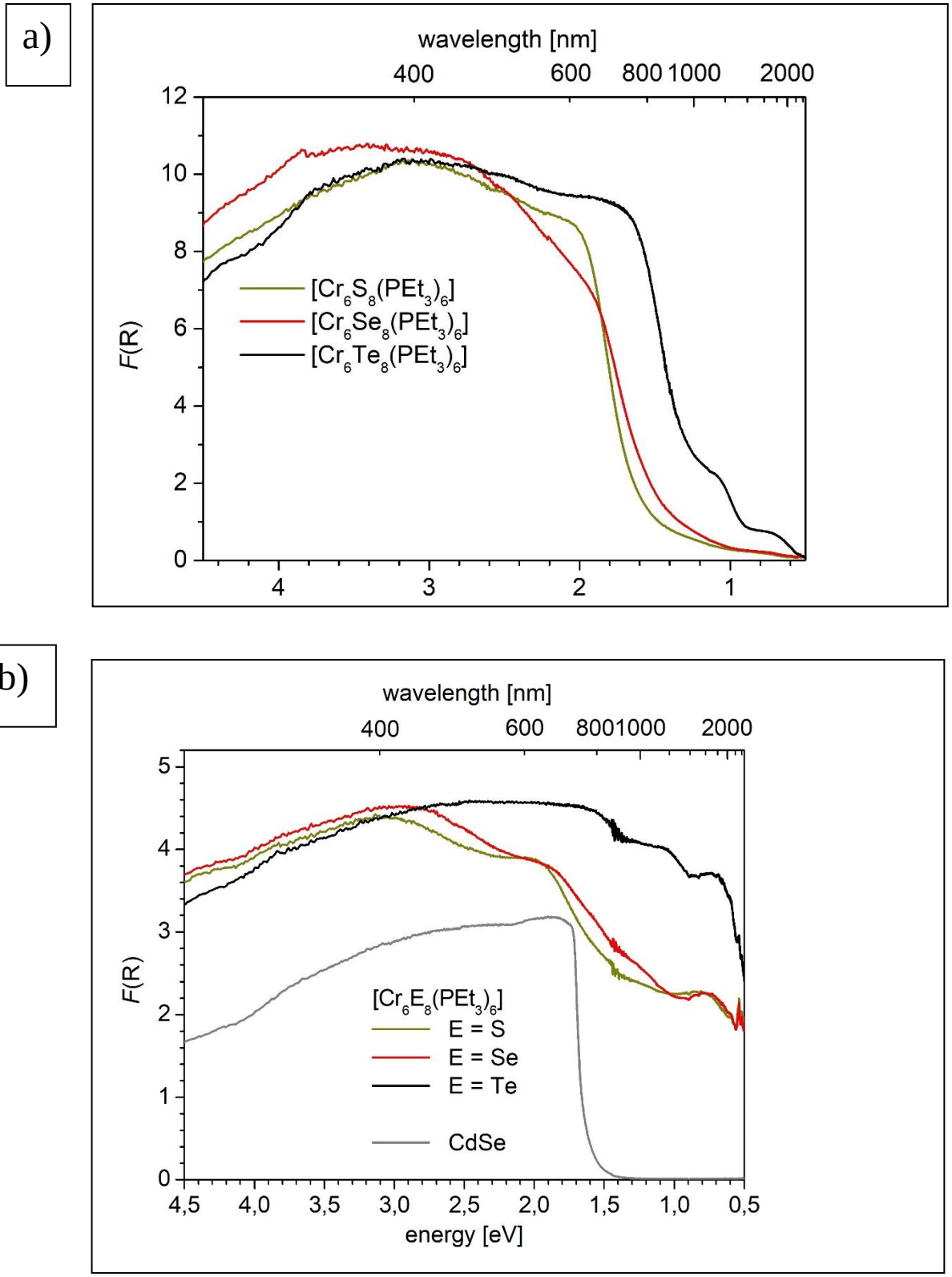

Figure S9. Reflection UV-Vis NIR spectra of **1a**, **2a** and **3** in solid state a) a mull in nujol and b) for microcrystalline powders in quartz cuvettes compared to the spectrum of CdSe.

a)

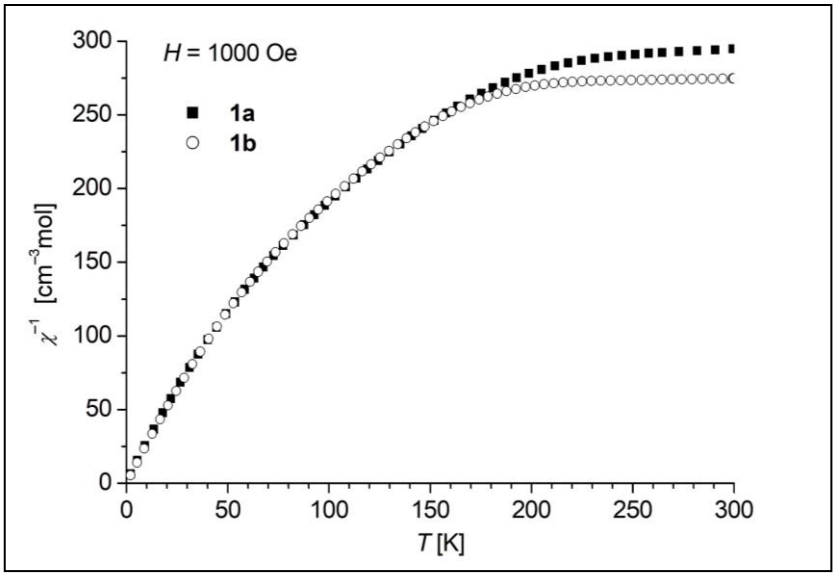

b)

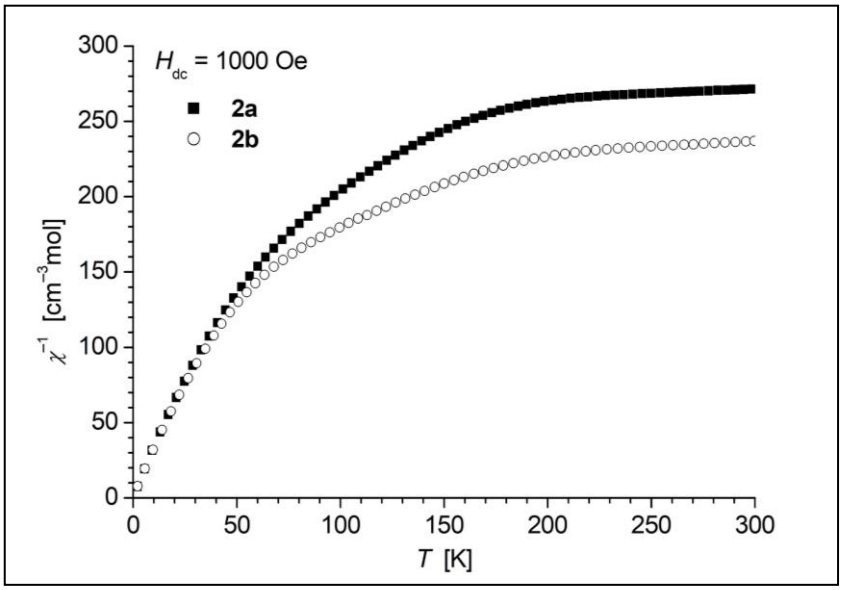

c)

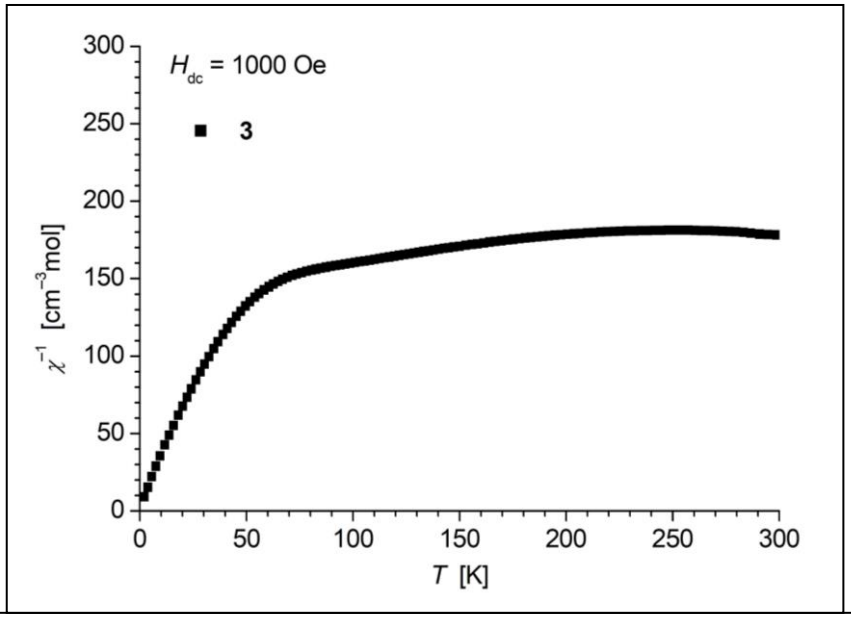

Figure S10 Temperature dependence of χ^{-1} of a) **1a** and **1b** b) **2a** and **2b**, c) **3.**

a)

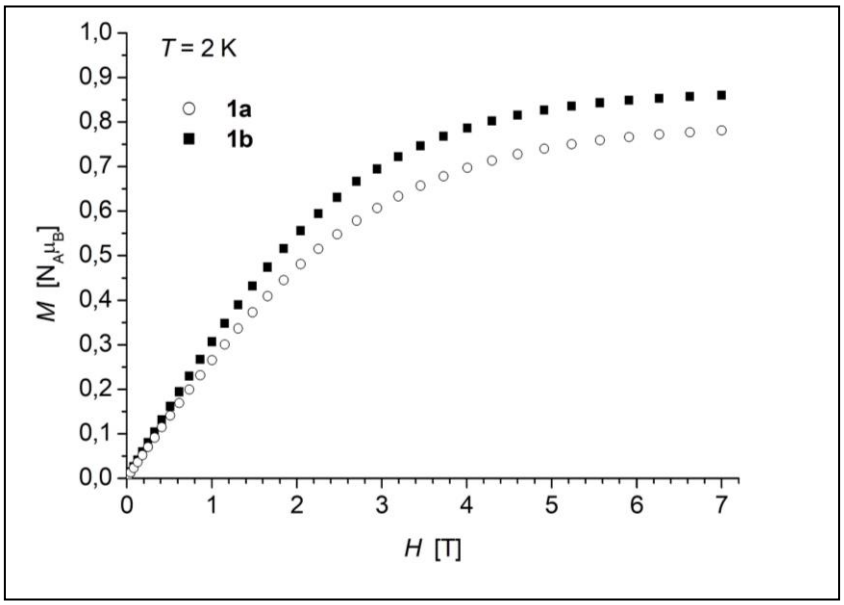

b)

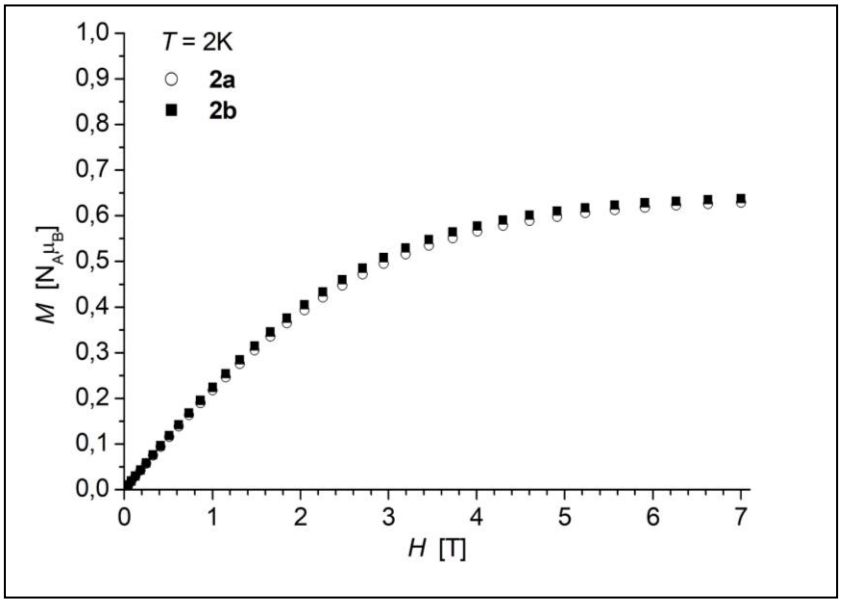

c)

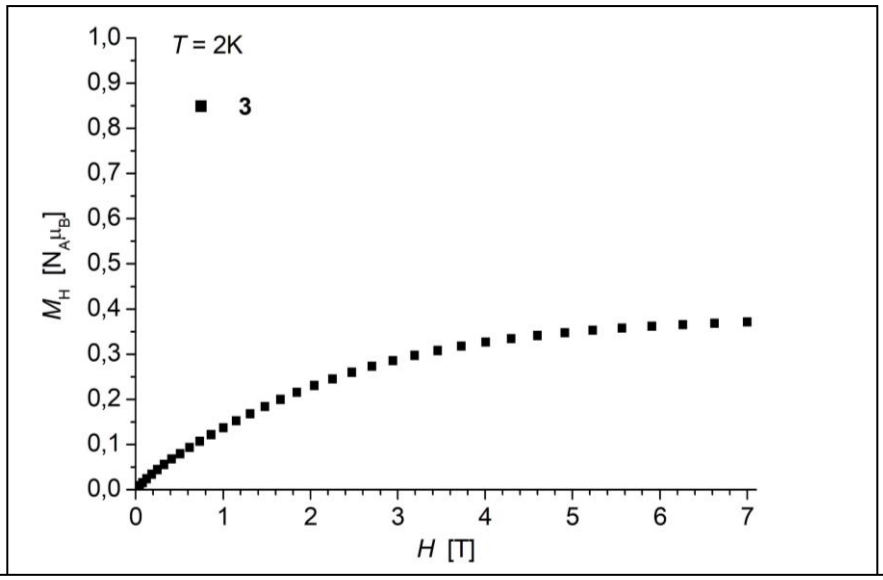

Figure S11 Magnetization curves at 2K of a) **1a** and **1b** b) **2a** and **2b**, c) **3.**

a)

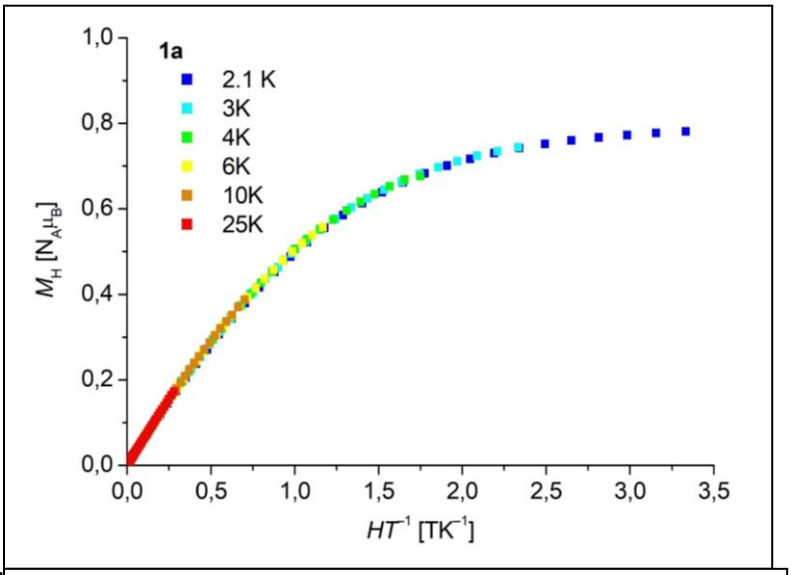

b)

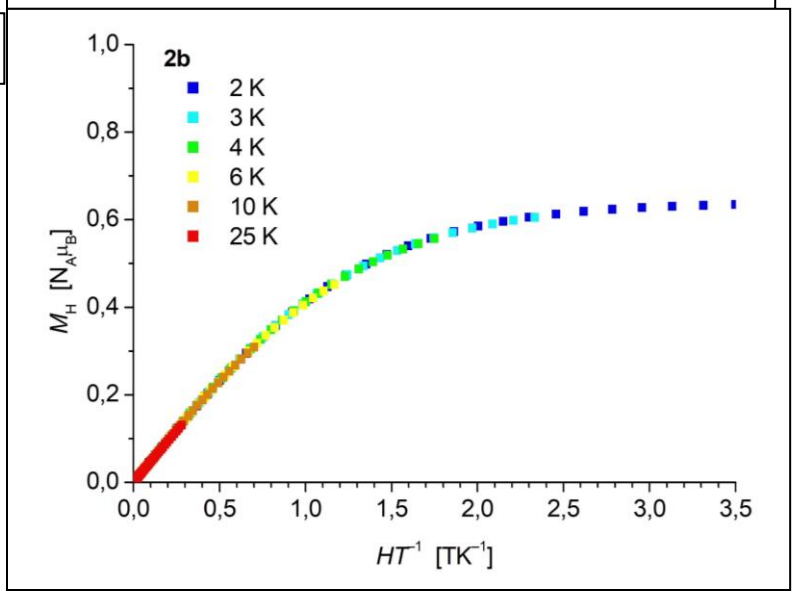

c)

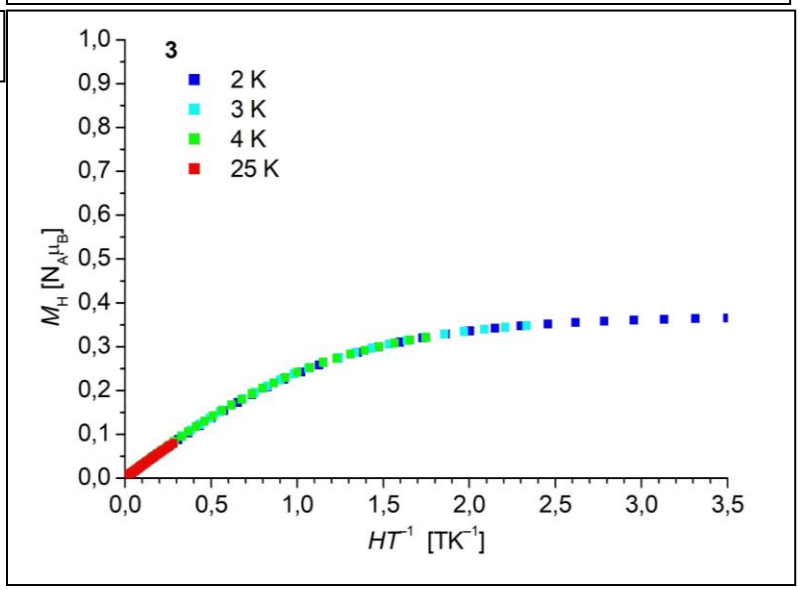

Figure S12 Plots of the reduced magnetization curves M vs HT^{-1} at different temperatures of a) **1a**, b) **2b** and c) **3.**

a)

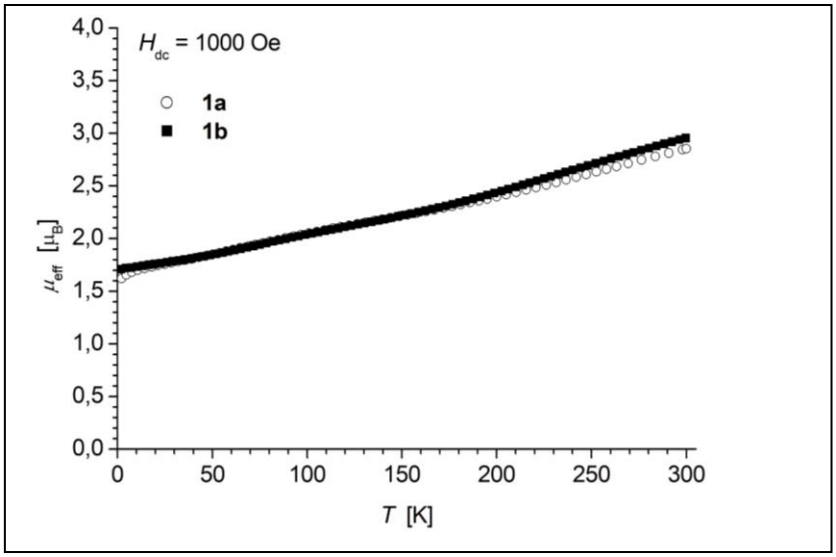

b)

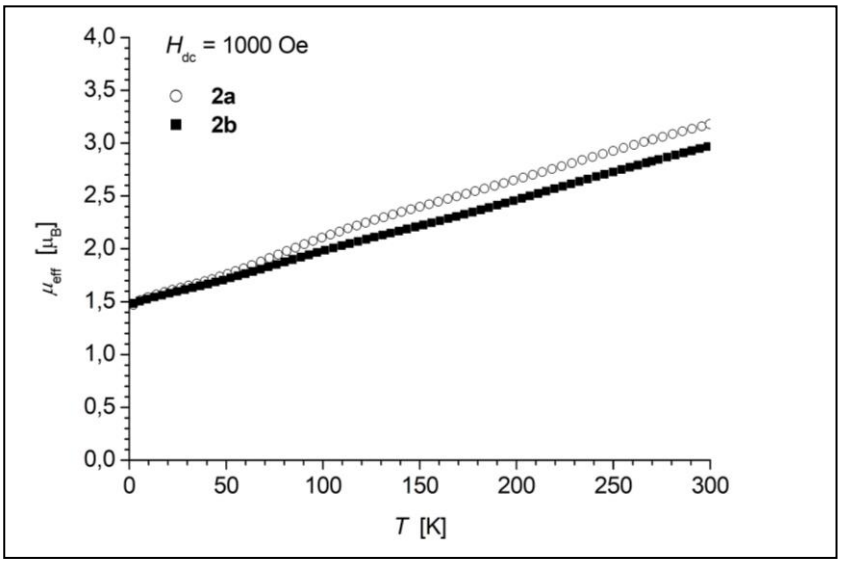

c)

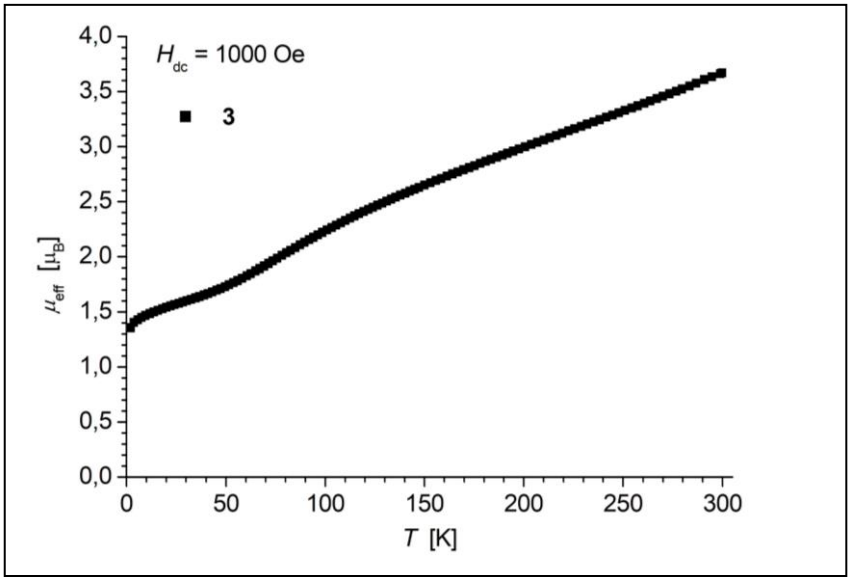

Figure S13 Magnetic moment μ_{eff} vs T for a) **1a** and **1b** b) **2a** and **2b**, c) **3.**

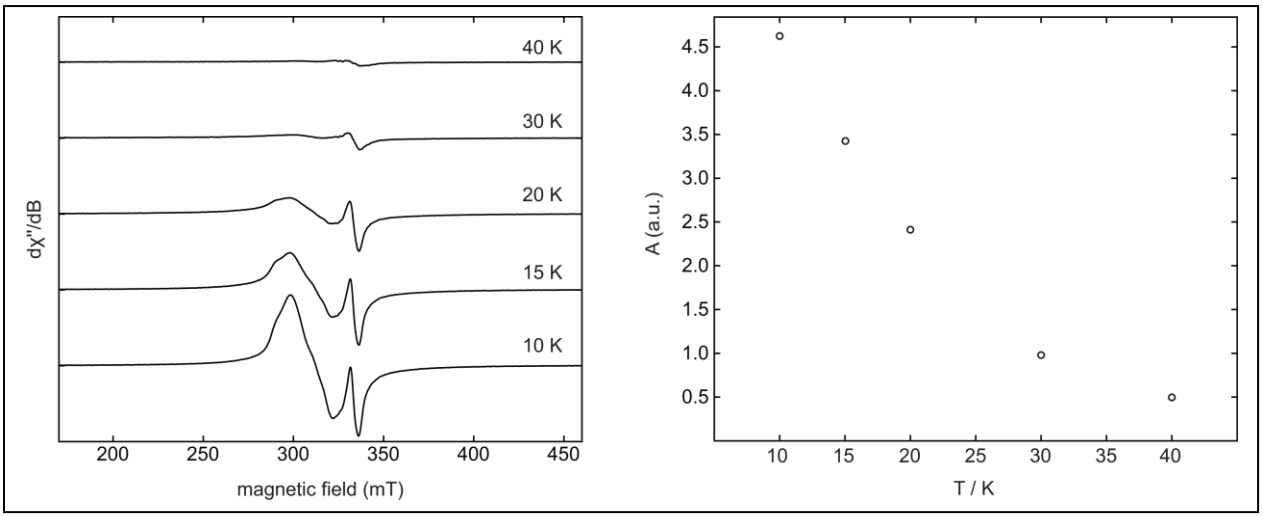

Figure S14 a) First-derivative EPR spectra of **1a** as a microcrystalline powder at various temperatures and b) temperature dependence of the double integral EPR intensity (*A*).

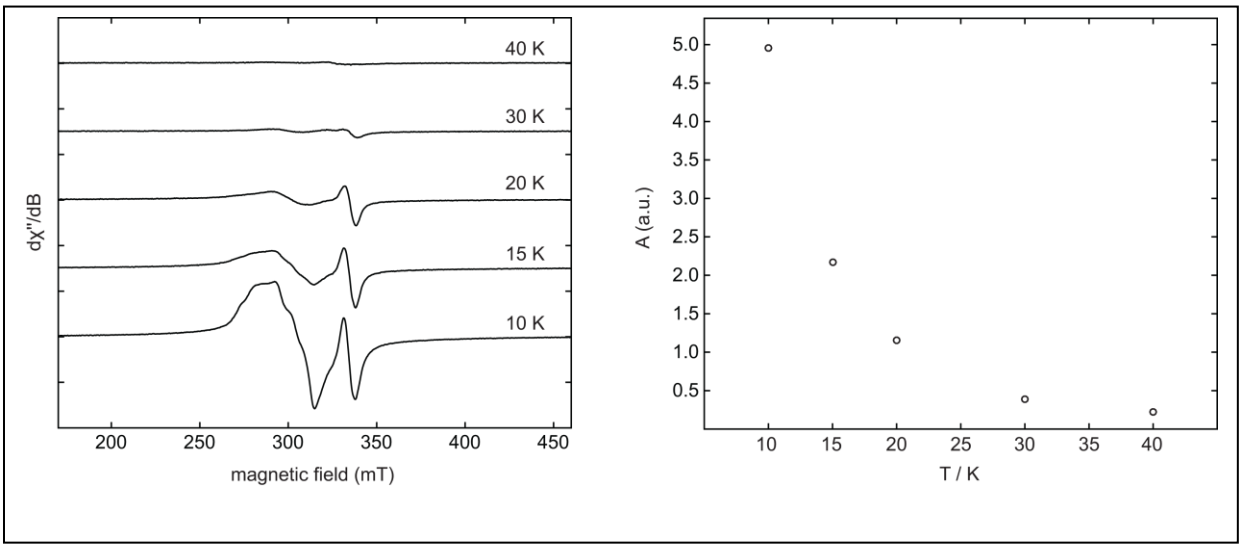

Figure S15 a) First-derivative EPR spectra of **2a** as a microcrystalline powder at various temperatures and b) temperature dependence of the double integral EPR intensity (*A*)**.**

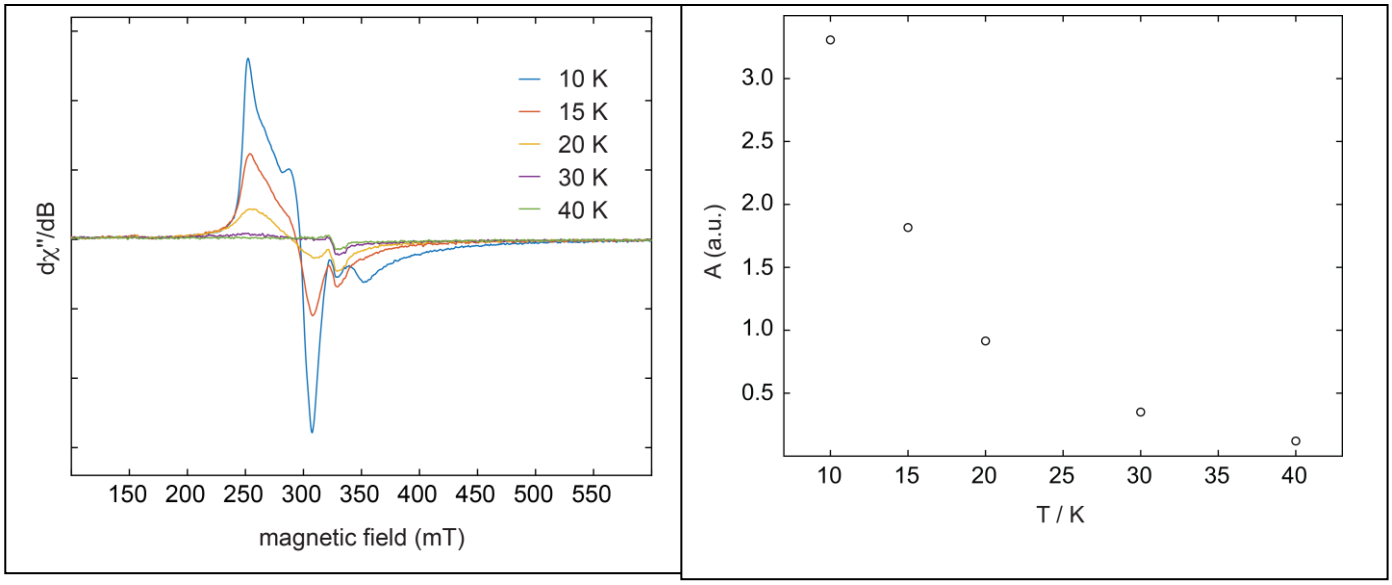

Figure S16. a) First-derivative EPR spectra of **3** as a microcrystalline powder at various temperatures and b) temperature dependence of the double integral EPR intensity (*A*)**.**

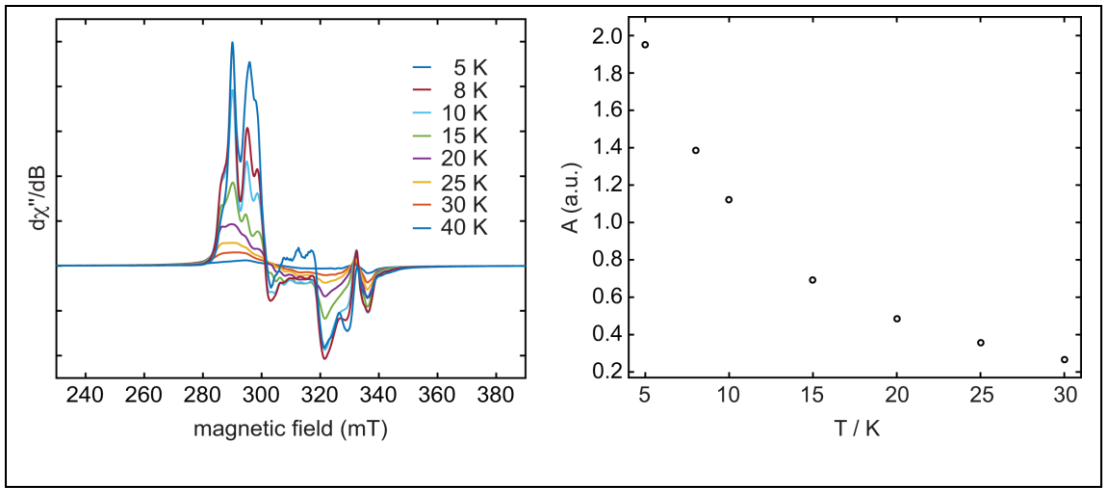

Figure S17 a) First-derivative EPR spectra of **1a** in frozen toluene at various temperatures and b) temperature dependence of the double integral EPR intensity (*A*)**.**

Table S4 Calculated bond energies [kJmol^{-1}] of hydrogen in the compounds $[M_6E_8(H)(PEt_3)_6]$ (M = Cr, Mo; E = S, Se) [a]

M	E	ΔE_1 [b]	ΔE_2 [c]
Cr	S	–243.2	–48.5
Cr	Se	–270.6	–103.2
Mo	S	–231.9	–26.0
Mo	Se	–253.7	–69.6

[a] (PBE/def2-TZVP)

[b] $\Delta E_1 = E(M_6E_8H(PEt_3)_6) - E(M_6E_8(PEt_3)_6) - E(H)$

[c] $\Delta E_2 = 2E(M_6E_8H(PEt_3)_6) - 2E(M_6E_8(PEt_3)_6) - E(H_2)$

Table S5 Calculated mean Cr···Cr distances [pm] in **1** and **2** [a]

	1			
	PBE	PBE0	B3LYP	exp. (120 K)
S = 0	248.57±0.12	244.82±0.06	248.29±0.04	256.74±0.73
S = 1	252.49±1.96	280.19±13.35	286.31±13.10	
S = 2	254.77±2.56	283.83±4.17	290.87±4.27	
	2			
S = 0	254.14±0.10	250.47±0.04	254.03±0.12	263.55±0,68
S = 1	256.62±3.50	290.20±11.46	298.25±11.80	
S = 2	268.91±4.09	294.92±4.00	304.52±4.21	

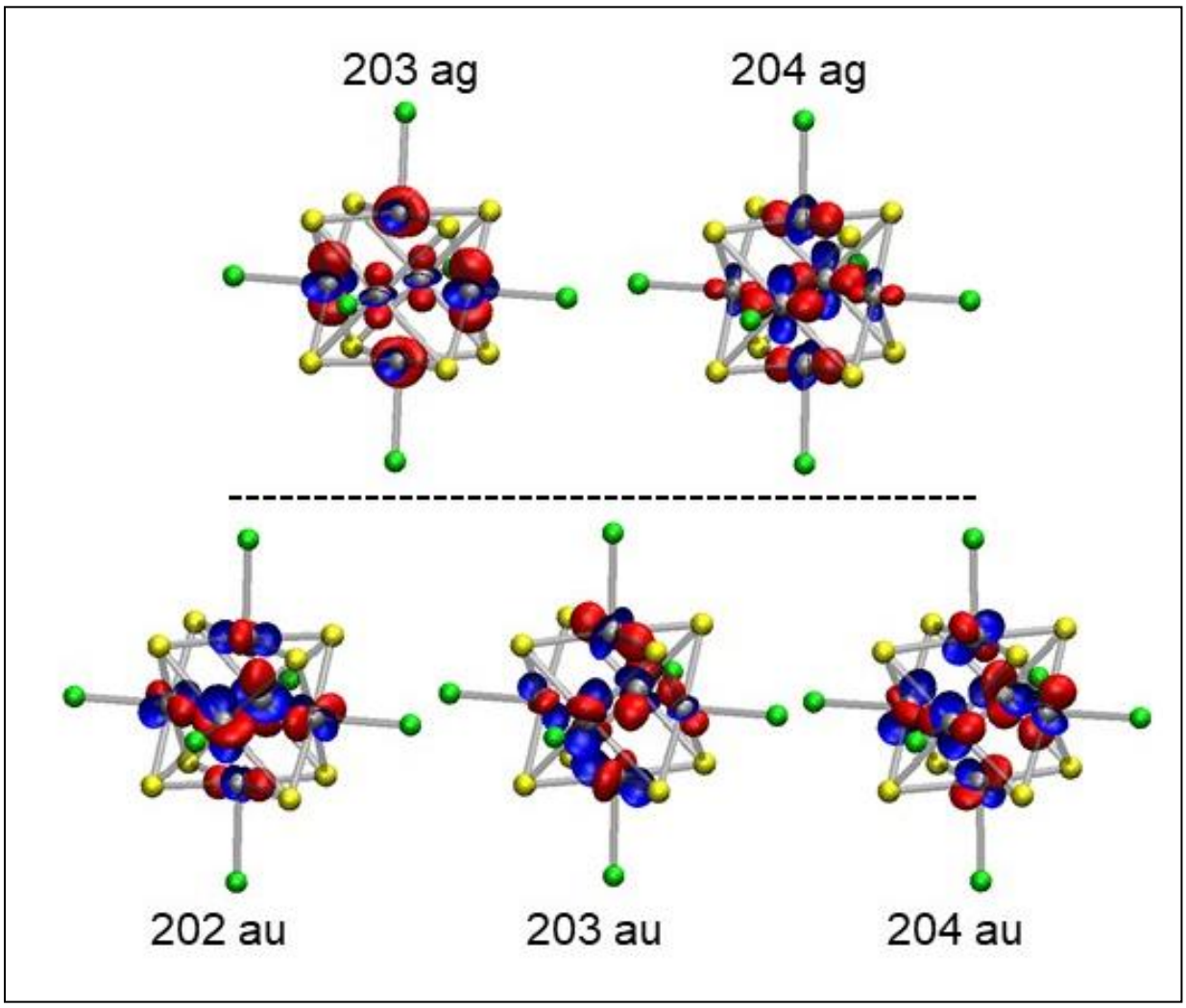

Fig. S18 Molecular frontier orbitals of **2** (occupied in the lower row, unoccupied in the upper row). Contours are drawn at 0.06 (red) and −0.06 (blue) atomic units [a.u.].

Table S6 Contributions of Cr, S, Se, and P atoms to the molecular HOMO and LUMO orbitals of **1** and **2** from Mulliken population analysis.[a]

$[Cr_6S_8(PEt_3)_6]$ (**1**)					
orbital		energy	S	Cr	P
+1	$168a_g$	–0.122	0.37	1.60	-
LUMO	$167a_g$	–0.122	0.37	1.60	-
HOMO	$168a_u$	–0.146	0.63	1.13	0,16
–1	$167a_u$	–0.146	0.65	1.12	0,14
–2	$166a_u$	–0.146	0.66	1.12	0.15
–3	$165a_u$	–0.149	0.17	1.72	-
–4	$164a_u$	–0.149	0.17	1.72	-
–5	$163a_u$	–0.149	0.19	1.72	-

$[Cr_6Se_8(PEt_3)_6]$ (**2**)					
orbital		energy	Se	Cr	P
+1	$204a_g$	–0.121	0.40	1.54	-
LUMO	$203a_g$	–0.121	0.41	1.54	-
HOMO	$204a_u$	–0.147	0.24	1.64	-
–1	$203a_u$	–0.147	0.28	1.60	-
–2	$202a_u$	–0.147	0.31	1.57	-
–4	$201a_u$	–0.148	0.56	1.26	0.11
–5	$200a_u$	–0.148	0.61	1.20	0.10
–8	$199a_u$	–0.149	0.59	1.23	0.11

[a] the total Mulliken population for each orbital amounts to 2 (= orbital occupation number).

Table S7 Lowest energy and dipole active singlet transitions in **1** and **2** [a,b]

$[Cr_6S_8(PEt_3)_6]$ (**1**)				$[Cr_6Se_8(PEt_3)_6]$ (**2**)			
	ΔE	f			ΔE	f	
1au	0,67987	4,30486E-5	H+0>L+0 (0.65) H-1>L+0 (0.13)	1au	0,71252	3,10733E-05	H+0>L+0 (0.38) H-2>L+0 (0.21) H-1>L+1 (0.13) H+0>L+1 (0.12)
2au	0,68155	3,64301E-5	H+0>L+1(0.49) H-2>L+0 (0.23) H-1>L+1 (0.10)	2au	0.71434	1,96453E-05	H-1>L+0 (0.31) H+0>L+1 (0.29) H-2>L+1 (0.19)
3au	0,68425	3,62048E-5	H-1>L+1 (0.43) H-2>L+0 (0.23) H-2>L+1 (0.16)	3au	0.71935	1,11923E-04	H-2>L+1 (0.26) H-4>L+0 (0.24) H-1>L+0 (0.23) H-5>L+1 (0.12)
4au	0,70625	0,00171	H-1>L+0 (0.42) H+0>L+1 (0.26) H+0>L+0 (0.12) H-1>L+1 (0.11)	4au	0.76003	5,26970E-04	H-4>L+0 (0.40) H-2>L+0 (0.23) H-1>L+1 (0.20)
5au	0,70729	0,00169	H-2>L+0 (0.38) H+0>L+1 (0.19) H-1>L+0 (0.15) H-1>L+1 (0.12) H+0>L+0 (0.12)	5au	0.76953	9,19305E-04	H-4>L+1 (0.59) H-5>L+0 (0.18)
6au	0,70988	0,00173	H-2>L+1 (0.61) H-1>L+1 (0.13) H-1>L+0 (0.11)	6au	0.77132	0.00104	H-5>L+1 (0.61) H-4>L+0 (0.12)
7au	0,77946	4,10046E-6	H-3>L+0 (0.55) H-5>L+0 (0.20)	7au	0.77486	0.00151	H-5>L+0 (0.61) H-4>L+1 (0.19)
8au	0,78052	3,27237E-6	H-3>L+1 (0.36) H-4>L+0 (0.20) H-4>L+1 (0.16) H-5>L+1 (0.15)	8au	0.78312	0.00113	H-8>L+0 (0.80)
9au	0,78315	2,6985E-5	H-5>L+1 (0.30) H-4>L+1 (0.29) H-5>L+0 (0.20) H-4>L+0 (0.12)	9au	0.78737	0.00121	H-8>L+1 (0.84)
10au	0,99738	7,27851E-4	H-4>L+0 (0.43) H-5>L+0 (0.25) H-4>L+1 (0.13)	10au	0.94599	5,26699E-04	H+0>L+0 (0.35) H-2>L+0 (0.14) H-8>L+0 (0.11)

[a] calculated by TDDFT with the PBE functional.

[b] notification, energy ΔE [eV], oscillator strength f, involved orbitals.

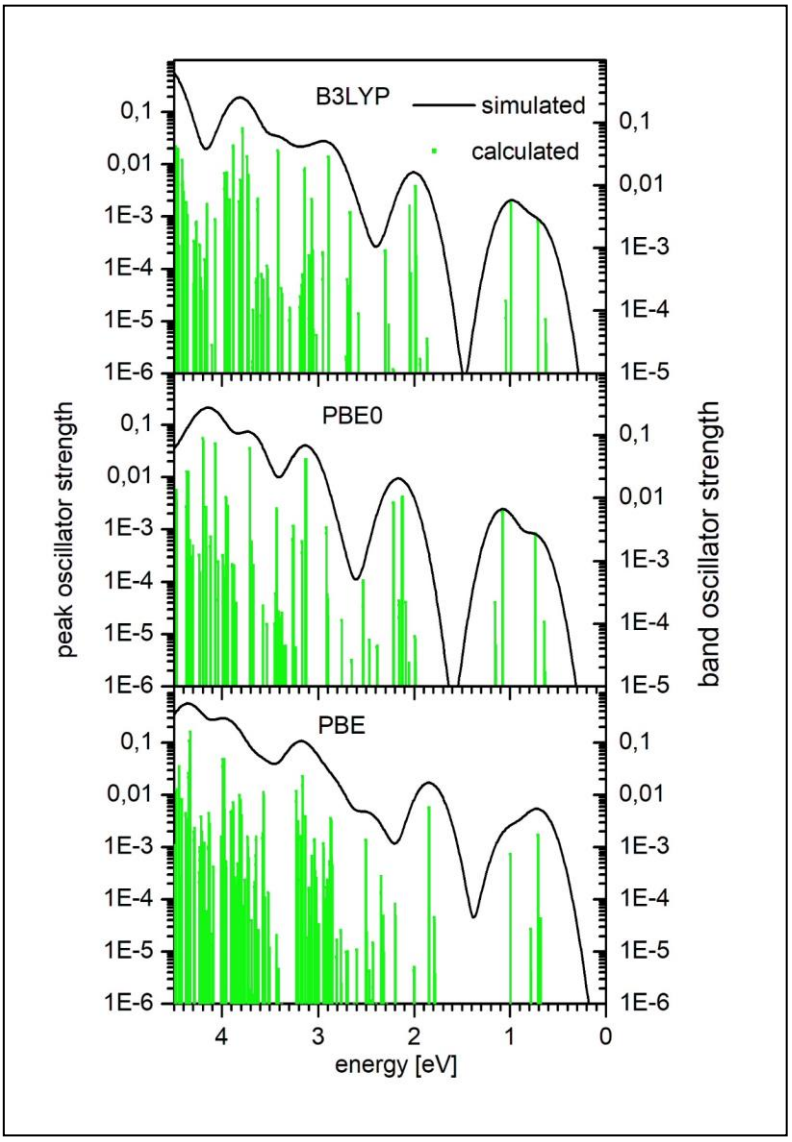

Figure S19. Calculated (TDDFT) electronic spectra of **1** calculated with three different functionals on log scales (B3LYP, PBE0, and PBE from top to bottom). Simulated spectra (black line) with superimposed Gaussians of FWHM = 0.3 eV were obtained from the calculated singlet excitation energies (green lines).

Table S8 Calculated energy differences ΔE [a] [kJ mol^{-1}] in **1** and **2** of the $S = 1$ and $S = 2$ states [b] to the $S = 0$ state

	1		**2**	
	$S = 1$	$S = 2$	$S = 1$	$S = 2$
ΔE (PBE)	30.5	38.8	25.9	–2.43
ΔE (PBE0)	–432.8	–658.0	–514.6	–746.8
ΔE (B3LYP)	–387.1	–591.0	–470.7	–681.8

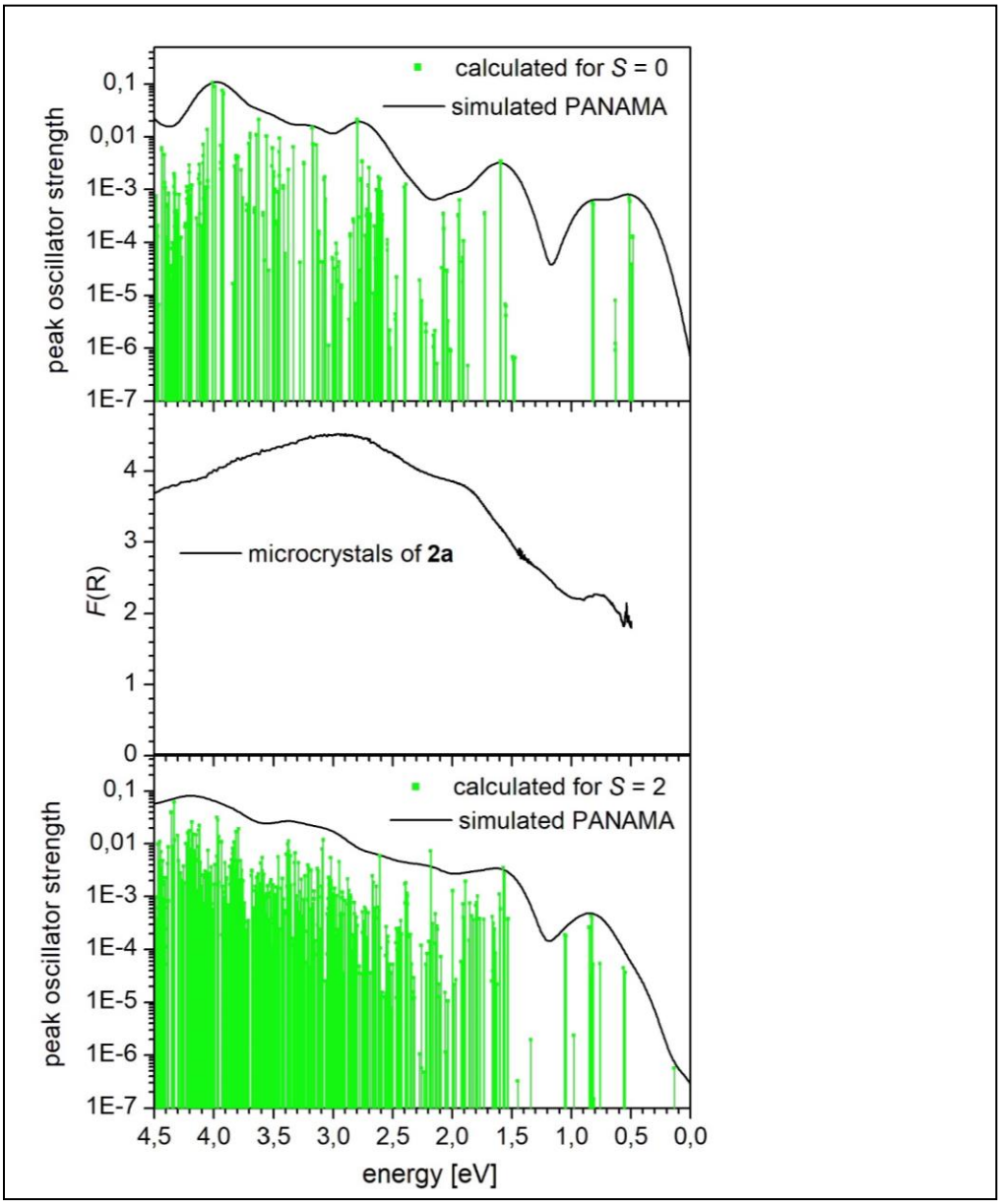

Figure S20. Experimental (powdered crystals in mineral oil) and calculated (TDDFT) electronic spectra of **2**. Panels up and down: calculated singlet excitation energies and oscillator strengths (green lines) on log scales and simulated spectra with superimposed Gaussians of FWHM = 0.3 eV for the closed shell state (S = 0) and the 2nd excited state (S = 2) of **2**; the middle panel displays the reflection spectrum of microcrystals of **2a**.